

# The influence of micro-formation on the in-plane elastic behaviour of paper

K. SCHULGASSER\*, Z. GRUNSEIT‡

\**Pearlstone Center for Aeronautical Engineering Studies, Department of Mechanical Engineering, Ben-Gurion University of the Negev, Beer Sheva, Israel*

‡*Mechanical Engineering Department, Radar Division, Elta Electronics Ltd, (Israel Aircraft Industry), Ashdod, Israel*

The in-plane stiffness of a paper sheet decreases as the amount of interfibre bonding is reduced. Part of this reduction has been explained in the past as due to the absence of stress in the constituent fibrous material in directions transverse to the fibre axis in a lightly bonded sheet. A model is offered to explain how the remaining reduction of stiffness for lightly bonded sheets is dependent on the uniformity of mass distribution, i.e., the formation, of the sheet. The theory is shown to be consistent with reported experimental results.

## 1. Introduction

Much progress has been made in the past 30 years in understanding the in-plane elastic behaviour of paper. We wish to predict this behaviour knowing the physical properties of the individual fibres, and knowing the geometry of the fibres and of their arrangement in the sheet. From the early, and seminal, simple network theories of Cox [1] and LaCacheux [2] mathematical models have evolved which include effects such as finite fibre length, fibre curl, drying stresses, and bond elasticity [3–5]. All of these models assume a uniform distribution of mass density in the sheet, i.e., no account is taken of formation. It is the purpose of the present work to make an assessment of this influence. We will conclude that for a *well bonded* sheet formation effects should be secondary, but we will propose a model which predicts the fall-off of Young's modulus in *poorly bonded* sheets in terms of formation effects. This model will avoid examining the problem of strain transfer to an individual fibre from those surrounding it. The latter approach was successfully utilized by Page and Seth [5] to describe the influence a low relative bonding area has on paper stiffness. Their expression for the dependence of stiffness on relative bonded area showed very good agreement with their experimental findings. The extreme complexity of the geometry and hence of the local stress distribution in the neighbourhood of a fibre means that a simple "micro-formation" model such as will be proposed would seem to be worthwhile as an alternative, albeit more abstract, explanation of this phenomenon. The current model leads to an expression for the dependence of Young's modulus on relative bonded area of a form different from that of Page and Seth, but equally able to explain their experimental data. Both their theory and the present one recognize that the drop off in stiffness with decreasing relative bonded area is brought about by non-uniformity of the strain

field in the sheet, but whereas the Page–Seth theory considers non-uniformities in an individual fibre, the present theory sees the dominant effect on non-uniformities in the strain field as resulting from non-uniformity of the mass density of the sheet at a somewhat larger dimensional scale.

At the outset we point out that it has recently been shown that the in-plane stiffness of a sheet is greater in a well bonded sheet than in a poorly bonded sheet due to a mechanism which is operative even when the strain distribution in the fibres is completely uniform [6]. This is due to the fact that in a well bonded sheet the fibres are stressed in the plane of the sheet also in directions perpendicular to the fibre axes, a phenomenon neglected in simple network models. Considering the actual elastic behaviour of the fibre cell wall it was shown that this increase is as much as 25% compared to the stiffness predicted by a simple network model. The actual difference, however, in stiffness between a well bonded and a lightly bonded sheet is experimentally found to be somewhat greater than this value [5]. It has been indicated [6] that even in a relatively lightly bonded sheet an appreciable amount of forced transverse deformation of the fibres occurs; thus the fall off in stiffness as bonding is reduced cannot be explained by the above mechanism alone.

The mass density of paper is far from uniform. Instruments for determining the distribution of mass density and techniques for its quantification have been put forth by many investigators (see [7], p. 185 ff). The simplest representation of the variation of mass density is obtained by subdividing a sheet into a checker-board of inspection squares of side length  $a$ . The variance of the mass density can then be experimentally determined as a function of  $a$ . Clearly if  $a$  is large the variance will approach zero. Such variances have been determined as a function of inspection square size. Corte [8] for instance has published this

type of data for 24 different papers. For the smallest square he considered, 1 mm, the largest coefficient of variation he found was 0.18. (The coefficient of variation is defined as the square root of the variance of mass density divided by the mean mass density of the sheet.) As the size of the inspection zone increases the coefficient of variation rapidly falls off. Clearly the local stiffness of the sheet is greater in areas where the mass density is greater. In fact it is reasonable to assume that the local elastic stiffness is proportional to local mass density. This is the outcome of the basic network theories, and if not precisely true for finite length fibres, should at least be a very good first approximation. We are thus confronted with the problem of determining the effective in-plane stiffness of a thin elastic sheet when the local stiffness is a random function of position in the sheet. If the effective stiffness were exactly equal to the global average of the local stiffness then the various theories for predicting sheet stiffness, although developed for uniform mass densities, would be applicable in the current instance also. However effective stiffness can rigorously be shown to be always lower than the global average stiffness. Any non-uniformity of mass density thus causes some reduction in stiffness. This reduction is, however, quite small if the coefficient of variation of the mass density (and hence of the local stiffness) is small.

## 2. Sheet with varying stiffness

For the current discussion it is convenient to define stiffness in terms of the in-plane shear modulus, denoted by  $G$ , and the plane stress area modulus, denoted by  $K$ . These are related to the in-plane Young's modulus  $E$  and in-plane Poisson ratio by

$$E = \frac{4KG}{K+G} \quad \nu = \frac{K-G}{K+G} \quad (1a, b)$$

For a sheet with varying stiffness, but which is statistically homogeneous and isotropic it is easily shown that rigorous bounds on the global effective values of the shear modulus and plane stress area modulus,  $G^*$  and  $K^*$  respectively, are given by

$$\left\langle \frac{1}{G} \right\rangle^{-1} \leq G^* \leq \langle G \rangle \quad (2)$$

$$\left\langle \frac{1}{K} \right\rangle^{-1} \leq K^* \leq \langle K \rangle \quad (3)$$

Here  $\langle \rangle$  denotes global area average. These results are easily derived from the classical principles of potential and complementary energy [9]. Up to second-order moments in  $G$  and  $K$  these bounds are simply

$$\langle G \rangle \left( 1 - \frac{\text{var } G}{\langle G \rangle^2} \right) \leq G^* \leq \langle G \rangle \quad (4)$$

$$\langle K \rangle \left( 1 - \frac{\text{var } K}{\langle K \rangle^2} \right) \leq K^* \leq \langle K \rangle \quad (5)$$

Here var denotes the variance. Beran [10] has pointed out that one can use perturbation techniques to determine effective global properties of heterogeneous materials. Such effective properties are not geometry

dependent up to the order of a linear term in the variance of the stiffness constants. We will determine effective stiffness up to this order by considering the two-phase case. Here we have only two materials constituting the statistically isotropic material; one has phase properties  $G_1$  and  $K_1$ ; the other has phase properties  $G_2$  and  $K_2$ . We define the phases such that  $G_1 \leq G_2$  and  $K_1 \leq K_2$ . (The combinations of material constants for which these two inequalities cannot simultaneously be satisfied will not be of interest to us.) Hashin [11] found bounds for the analogous generalized plane strain problem. A cursory examination of the analysis reveals that the bounds carry over to the case of plane stress if in his expressions the "plane strain bulk modulus" is replaced by the "plane stress area modulus". Then from Hashin's equations (4.25 to (4.28)

$$\begin{aligned} G_1 + \frac{v_2}{\frac{1}{G_2 - G_1} + \frac{(K_1 + 2G_1)v_1}{2G_1(K_1 + G_1)}} &\leq G^* \\ &\leq G_2 + \frac{v_1}{\frac{1}{G_1 - G_2} + \frac{(K_2 + 2G_2)v_2}{2G_2(K_2 + G_2)}} \quad (6) \\ K_1 + \frac{v_2}{\frac{1}{K_2 - K_1} + \frac{v_1}{K_1 + G_1}} &\leq K^* \\ &\leq K_2 + \frac{v_1}{\frac{1}{K_1 - K_2} + \frac{v_2}{K_2 + G_2}} \quad (7) \end{aligned}$$

Here  $v_1$  and  $v_2$  are the area fractions (volume fractions in the original formulation) of the two phases. We will be interested only in the case when both materials have the same Poisson ratio, and for simplicity only when  $v_1 = v_2 = 0.5$ , i.e., equal amounts of each phase. Then after some manipulation the bounds on  $G$  can be put into the form

$$\begin{aligned} \langle G \rangle \left[ 1 - \frac{\frac{1 + \nu \text{ var } G}{2 \langle G \rangle^2}}{1 - \left(1 - \frac{\nu}{2}\right) \left(\frac{\text{var } G}{\langle G \rangle^2}\right)^{1/2}} \right] &\leq G^* \\ \leq \langle G \rangle \left[ 1 - \frac{\frac{1 + \nu \text{ var } G}{2 \langle G \rangle^2}}{1 + \left(1 - \frac{\nu}{2}\right) \left(\frac{\text{var } G}{\langle G \rangle^2}\right)^{1/2}} \right] &\quad (8) \end{aligned}$$

$\nu$  is the common Poisson ratio of both materials. Here we have used the fact that for the case considered

$$\langle G \rangle = \frac{G_1 + G_2}{2} \quad \text{var } G = \frac{(G_2 - G_1)^2}{4}$$

The bounds on  $K$  are identical to the above if each  $G$  is replaced by  $K$ . Then to the linear term in variance we have

$$G^* = \langle G \rangle \left( 1 - \frac{1 + \nu \text{ var } G}{2 \langle G \rangle^2} \right) \quad (9)$$

and a similar expression is obtained for  $K$ . This is the geometry independent effective stiffness, valid for low

TABLE I Calculated stiffnesses for material shown in Fig. 1, together with the Hashin bounds.

$G_2/G_1$ and $K_2/K_1$	Hard Material Inclusion		Soft Material Inclusion		Hashin bounds <sup>†</sup>	
	$G^*$	$K^*$	$G^*$	$K^*$	$G^*$ Lower	$G^*$ Upper
	$\langle G \rangle$	$\langle K \rangle$	$\langle G \rangle$	$\langle K \rangle$	$\langle G \rangle$	$\langle G \rangle$
2	0.920	0.918	0.933	0.933	0.917	0.933
4	0.711	0.708	0.796	0.797	0.700	0.800
10	0.403	0.397	0.636	0.640	0.386	0.649
40	0.125	0.122	0.518	0.525	0.117	0.542
400	0.014	0.013	0.476	0.484	0.012	0.504

<sup>†</sup> same for  $K$

variances. It is easily seen from (1a) and (1b) that this expression is also valid for  $E$  and that to the order of the linear term in the variance, the Poisson ratio of the aggregate remains equal to the common Poisson ratio of the constituent materials. Equation 9 could also have been derived from the more general perturbation methods used by Silnutzer [12] for the plane strain problem.

We seek an approximate expression giving effective stiffness which depends only on the average stiffness and on the variance, and which is valid even for rather large variances. We can find a clue as to where to look if we consider that the bounds of Hashin (Equations 6 and 7) correspond to the effective stiffness of real two-phase materials (and thus his bounds are the best possible in terms only of the stiffness constants of the two constituting materials and of their area fractions). This was shown by Hashin to be true for  $K$  and only recently Milton [13] showed that the analogous expressions for  $G$  in the three-dimensional case represent realizable two-phase material geometries; hence for our two-dimensional case this is apparently also true. Hashin's lower bound on  $K$  corresponds to a material constructed as follows: consider a plane completely filled with composite discs, each disc having a core with material of constants  $G_2$  and  $K_2$  and an outer ring of material constants  $G_1$  and  $K_1$ . The ratio of the core diameter to the outer diameter of the ring is maintained constant such that the core always constitutes the area fraction  $v_2$  of the composite disc, and it is assumed that composite discs of all sizes are available so that in the limit the plane can be completely filled. The upper bounds are realized when the roles of the two materials are reversed. The essential "qualitative" feature of these two materials is that the stiffer (softer) material is clearly identified with convex inclusions which are well separated from each other while the softer (stiffer) material plays the role of the matrix. As an indication that these are the main geometrical features as far as influencing effective stiffness we have computed, using the finite element method (see Appendix A for details), the effective modulus of the material shown in Fig. 1 with  $\nu = 1/3$ . Due to the three-fold symmetry this material is globally isotropic; the triangular inclusions constitute 50% of the total area. The effective stiffness constants of this material are shown in Table I and compared with the Hashin bounds. The striking closeness of the results to the Hashin bounds is a strong indication of the importance of the inclusion-matrix geometry in determining

effective modulus. (It also constitutes strong circumstantial evidence as to the realizability of the Hashin bounds.) Now the distribution of mass density of paper does not show an inclusion-matrix feature. In fact visual examination of mass density maps of paper (from beta radiographs or light transmission) shows at least a subjective symmetry between light and dark areas. Hence in seeking our approximate expression for effective stiffness we sought a symmetric model. The simplest symmetric model with global isotropy is that shown in Fig. 2. Its effective stiffnesses were calculated using the finite element method (see Appendix A for details). The results for  $G$  are shown by the circles in Fig. 3. Also shown there are the Hashin bounds (Equation 8) and Expression 9 for the effective stiffness to linear terms in the variance. It is clear that for this symmetric model Equation 9 is not only valid for small variances, but is an excellent approximation even for large variances. The results for  $K$  and  $E$  lead to similar conclusions as to the validity of Equation 9 when  $G$  is replaced by  $K$  or  $E$ .

### 3. Application to paper

Let us apply the results of the last section to a paper sheet. As pointed out the largest coefficient of variation found by Corte [8] for 1 mm square inspection zones was 0.18. Now Poisson's ratio for paper is usually taken to be 1/3 or a bit less [14]; then the coefficient  $(1 + \nu)/2$  in Equation 9 is either 2/3 or slightly smaller. Hence if the variances as measured on zones of size 1 mm by 1 mm are representative of the true stiffness variances then we can expect stiffness reductions of no more than of the order  $(2/3)(0.18)^2$ . These are clearly insignificant. As pointed out earlier, however, variance increases as the inspection zone size

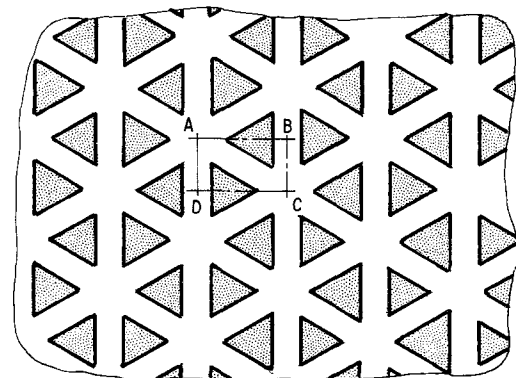


Figure 1 Model of material with well separated convex inclusions.

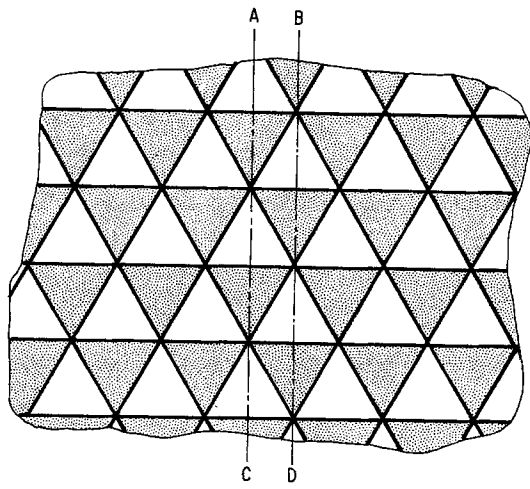


Figure 2 Model of symmetric material.

decreases. However, quite a large increase of variance would be necessary to produce a meaningful stiffness reduction. No matter how much we shrink the inspection zone we cannot find variances greater than the point variance. The point variance of stiffness (assuming as we have that "stiffness" is proportional to mass density) is proportional to the average number of fibres at the point (see [7], p. 202). Then

$$\frac{\text{var } G}{\langle G \rangle^2} = \frac{1}{\bar{n}} \quad (10)$$

where  $\bar{n}$  is average thickness of the sheet in terms of number of fibres. Since  $\bar{n}$  is usually 8 or more, even this would not constitute a significant stiffness reduction. We note that for extremely thin sheets the point coefficient of variation, which is an upper bound on the zonal coefficient of variation we have heretofore considered, can be quite high. We must of course question the validity of applying Equation 9 at size scales comparable to fibre width. Equation 9 is based on a continuum assumption; it is not at all clear

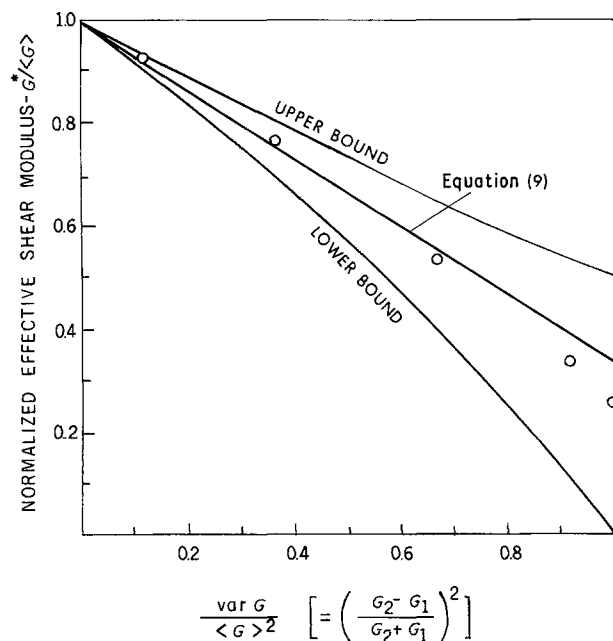


Figure 3 Comparison of the expression of Equation 9 with the finite element calculation of effective shear modulus of a symmetric material.

what is the minimum inspection size for which zonal variance could reasonably be put into Equation 9. However, based on the low variances involved one cannot *apparently* avoid the conclusion that effective stiffness of the sheet is very nearly the average of the local stiffness. This would be a valid conclusion were it not for another factor we have not yet considered.

It has been recognized for over twenty years that paper has a layered structure. This structural form was put forth by Kallmes and Corte [15], essentially as a mathematical device to facilitate their analysis of the statistical geometry of a paper sheet. Since then it has come to be well accepted that the actual physical structure and the behaviour of paper indicate strong layering, and it has been demonstrated that this layering is an inevitable outcome of the thickening and filtration process during the forming of the wet web [16]. We posit that the paper sheet can be modelled by thin layers "stitched" together by bonds. The individual layers of the sheet would have relatively very high mass density variance (and hence stiffness variances). If the "stitches" are spaced far apart relative to a statistical scale then the stiffness of the sheet would equal the average of the stiffness of the individual layers — i.e., exactly the layer stiffness if all layers are statistically identical. Then the sheet stiffness would be greatly reduced. If the "stitches" are very closely spaced then the average mass across the layers is the appropriate mass density from which variances are to be derived — and as has been pointed out, these are relatively small. As a simplistic illustration of this idea consider a sheet made up of two layers of the material shown in Fig. 2. Place one layer over the other such that the white triangles of one coincide with the shaded triangles of the other. Were the two layers continuously glued together or "stitched" at a spacing small compared to triangle size then sheet stiffness would be simply the average stiffness of the "white" and "shaded" materials. If, however, the stitching was at a scale large compared to triangle dimensions the sheet stiffness would be equal to layer stiffness (i.e., reduced from the nominal average stiffness) as this is calculated from Equation 9. For a paper sheet (or its layers) the mass density (local stiffness) variance increases at small zone sizes. Hence we can conceive of the process just described taking place on a continuous basis. The closer is the "stitching" the lower is the "effective" variance of the sheet. Now the relative bonded area (RBA) of a sheet of paper is defined as that fraction of the total upper and lower surface of the fibres which is bonded to another fibre surface. As the relative bonded area of a sheet increases the bond density will increase, i.e., the bonds will be more closely spaced. The simplest assumption relating relative bonded area to a zone size for which adjacent layers can be assumed to be knitted together would be to take the side length squared of such a zone size to be proportional to the relative bonded area, i.e.,

$$\text{RBA} \propto a^2$$

or

$$a \propto (\text{RBA})^{1/2} \quad (11a)$$

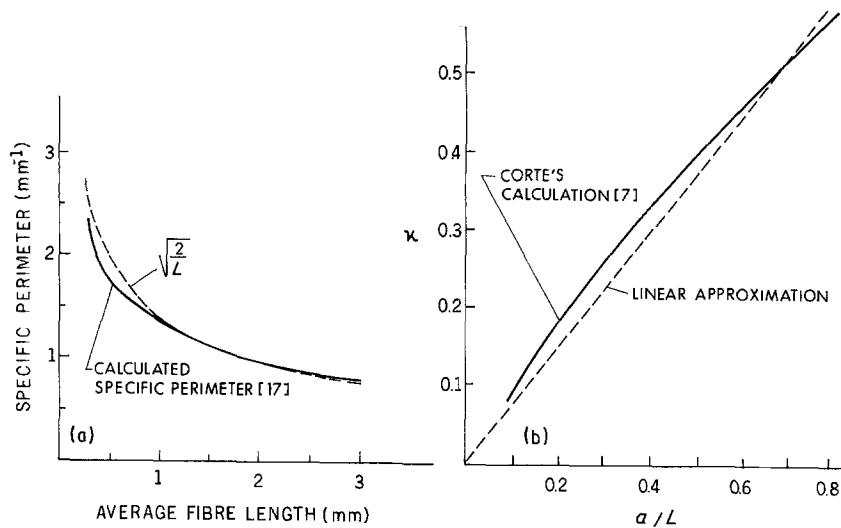


Figure 4 (a) Calculated and approximate dependence of specific perimeter on average fibre length. (b) Calculated and linear approximation for the factor  $\kappa$  as it depends on the ratio of inspection zone size to fibre length.

The implication of this assumption is that as the RBA increases the number of bonding sites increases proportionately, their spacing becoming denser. In other words we are saying that there is a threshold area on the interlayer surface which must be bonded in order to guarantee that the layers work together. We can also determine the nature of the dependence of  $a$  on fibre length. Jordan and Nguyen [17] have calculated "specific perimeter" for a random sheet. They point out that specific perimeter is a measure of how fine-grained the formation texture is. Its reciprocal would be a measure of the scale of the texture. Using  $30 \mu\text{m}$  as mean fibre width with standard deviation of  $4 \mu\text{m}$  their Fig. 11 shows specific perimeter as a function of average fibre length,  $L$ . Their computation involves a numerical procedure but a very close approximation to the result is given by

$$\text{specific perimeter} \propto \frac{1}{L^{1/2}}$$

(see Fig 4a). Jordan [18] has verified this behaviour for length distributions other than that of the previously cited reference. Thus the scale of the texture is proportional to  $L^{1/2}$  and we take

$$a \propto L^{1/2} \quad (11b)$$

Now the variance of average mass density in an inspection zone of an ideal network of fibres is given by [19]

$$\frac{\text{var } W^*}{W^2} = \kappa \frac{L\omega}{a^2} \quad (12)$$

where  $L$  is the fibre length,  $\omega$  the fibre width, and by the assumed linear relationship between local mass density and local stiffness the left-hand side is also the coefficient of variation of the stiffness.  $\kappa$  is a non-dimensional factor dependent on the ratio  $a/L$ . The range of  $a$  of interest to us is from somewhat more than fibre-to-fibre crossing distance up to somewhat less than fibre length. Using Corte's expression for  $\kappa$  it is found that for  $0.1 < a/L < 0.8$  (see Fig. 4b)  $\kappa$  can be taken, as a very good approximation, to be proportional to  $a/L$ . In reality Corte's experiments [8] have shown that variance of *real* papers are greater than those predicted by Equation 12, but there is no reason to expect that the nature of the dependence on  $L$ ,  $\omega$  and  $a$  is radically altered. Then Equation 12 gives

$$\frac{\text{var } W^*}{W^2} \propto \frac{\omega}{a} \quad (13)$$

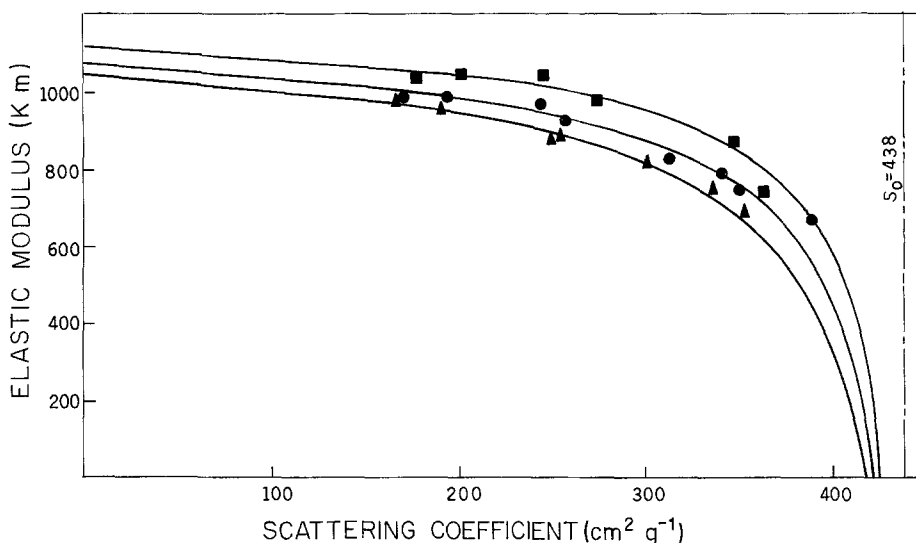


Figure 5 Elastic modulus plotted against scattering coefficient for sheets made of the same pulp with different average fibre length (■ 2.01 mm, ● 1.41 mm, ▲ 1.10 mm). Curves are fitted to Equation 17 using  $\langle E \rangle = 1310 \text{ km}$ ,  $S_0 = 438 \text{ cm}^2 \text{g}^{-1}$ ,  $C = 0.223 \text{ mm}^{1/2}$ . The modulus is normalized by the mass density of the sheet and reported in the traditional "length" unit, km.

and from Equations 11a and 11b, recalling our assumption that local elastic stiffness is proportional to local mass density, we conclude that

$$\frac{\text{var } G}{\langle G \rangle^2} \propto \frac{1}{(L \cdot \text{RBA})^{1/2}} \quad (14)$$

and using Equation 9 we can finally write, in terms of the Young's modulus,

$$E^* = \langle E \rangle \left( 1 - \frac{C}{(L \cdot \text{RBA})^{1/2}} \right) \quad (15)$$

where  $C$  is some constant. This form for the dependence of effective stiffness shows the same tendencies as that suggested by Page and Seth, and we will see that it is equally consistent with their data.

#### 4. Comparison with experimental results

Optical scattering coefficient of a sheet is generally taken to be a measure of the relative bonded area in the form [5]

$$\text{RBA} = \frac{S_0 - S}{S_0} \quad (16)$$

where  $S$  and  $S_0$  are the optical scattering coefficients of the sheet and of the fibres (in their unbonded state) respectively. Equation 15 then becomes

$$E^* = \langle E \rangle \left( 1 - \frac{C(S_0)^{1/2}}{[L(S_0 - S)]^{1/2}} \right) \quad (17)$$

By appropriately choosing the parameters  $\langle E \rangle$ ,  $C$  and  $S_0$  this expression can be made to fit quite well all of the data for  $E^*$  as a function of  $S$  reported by Page and Seth [5]. In these experiments fibre length was not controlled. However, a more discriminatory set of data is that subsequently reported by them [20]. Here fibre length was varied by preparing a series of pulps from guillotined handsheets so that fibre length varied while all other properties remained constant. A fit of Equation 17 to this data is shown in Fig. 5. The equation is clearly seen to be consistent with the data. We should point out that the fit is not better than that found by Seth and Page using the relationship derived from their theory. Their expression is

$$E^* = \frac{E_f}{3} \left( \frac{C S_0}{L(S_0 - S)} \tanh \frac{L(S_0 - S)}{C S_0} \right) \quad (18)$$

Where  $E_f$  is the axial Young's modulus of the fibre. The fit of the data to either equation predicts nearly identical values of  $S_0$ . Hence both place any particular data point at the same RBA. It is not our purpose to compare the two theories and determine which is "better". Each certainly represents a gross simplification of the actual strain distribution in the sheet. Quite likely both mechanisms come into play, i.e., diminution of the strain in individual fibres near their ends, and diminution of the local strain below the average strain in the sheet at a larger dimensional scale due to inevitable non-uniformities of mass distribution whose effect is accentuated by low relative bonded area. Which is the dominant mechanism is not

clear at this point. Some obvious limitations of the present theory must be pointed out. It cannot be expected to be applicable at very high or very low RBA since here the approximations 11a and 11b would not be expected to hold. It is however interesting to note an implication, probably fortuitous, of Equation 17. That expression implies that the elastic modulus should drop to zero at some finite RBA over 0. In other words it is predicting a threshold RBA below which a connected network of fibres will not be formed. For the data just considered, such thresholds are predicted to be 2.6%, 3.7% and 4.7% for fibre lengths of 2.01, 1.41 and 1.1 mm respectively.

#### 5. Conclusions

Equation 15 shows the manner in which Young's modulus depends on relative bonded area and fibre length due to the influence of mass non-uniformity of the sheet. This influence is magnified as RBA is reduced. As fibre length increases the influence of RBA is decreased; for infinitely long fibres the effective Young's modulus is not reduced from the average modulus of the sheet. As was indicated earlier, the mass non-uniformity should not appreciably influence the Poisson ratio. We have already pointed out that the effect considered here is not the only one acting to reduce paper stiffness. At a smaller geometrical scale the inability of fibre ends to achieve strain levels globally present in the sheet will also reduce stiffness. This effect was modelled by Page and Seth [5]. As the relative bonded area decreases, the "laminar" effect which stiffens the sheet by inducing transverse fibre strains will become less effective [6].

We close by pointing out that in order to examine the effect of mass density variations coupled with low RBA on elastic stiffness it was necessary to construct a model of sufficient simplicity so as not only to be mathematically viable but also to contain a small enough number of undetermined parameters so that comparison with experimental results can be seen as a corroboration of the suggested mechanism rather than simply as a curve-fitting exercise, thus the "layered" model is used. The layering of paper is not the discrete phenomenon implied in the present model, but is rather an expression of the strong tendency of the fibres to be parallel to the sheet plane and not to be "felted", that is not to be interwoven. It might be appropriate here to quote the words of Corte ([7], p. 273) in discussing a model due to Scallan and Borch [21] to explain the optical properties of paper: "The approach is reminiscent of the multilayer approach to the porous structure of paper . . . and it has the same weakness, namely, the uncertainty of the definition of a layer . . . . The usefulness of such an approach does not necessarily depend on whether the model can be shown to be real but on the extent to which one can use it as a crutch to arrive at a goal that is quite independent of the construction of the crutch."

#### Appendix A

The strain energy contained in some area  $A$  of an

elastic sheet of unit thickness in plane stress is given by

$$U = \int_A \left( \frac{K}{2} (\varepsilon_x + \varepsilon_y)^2 + G [2\varepsilon_{xy}^2 + \frac{1}{2}(\varepsilon_x - \varepsilon_y)^2] \right) dA \quad (A1)$$

Where  $\varepsilon_x$  and  $\varepsilon_y$  are normal strains in the  $x$  and  $y$  directions respectively and  $\varepsilon_{xy}$  is the shear strain. Consider the following in-plane displacement system imposed on the boundary of a sample of an elastic sheet

$$\begin{aligned} u &= bx \\ v &= by \end{aligned} \quad (A2)$$

where  $b$  is a constant,  $u$  the displacement in the  $x$  direction and  $v$  in the  $y$  direction. Such displacements imposed on the boundary of a material with uniform elastic properties would produce a uniform strain field. The strain energy in the sample would be

$$U = 2KbA \quad (A3)$$

where  $K$  is the constant area modulus of the material. However, if the sample had varying stiffness, and further if the sample were large compared to the geometry of the microstructure and if the phase geometry is such that the overall mechanical behaviour is isotropic then the displacements imposed on the boundary would result in strain energy

$$U = 2K^*bA \quad (A4)$$

where  $K^*$  is the effective area modulus of the sample (see [9], p. 39 for a formal proof in the three-dimensional case). Thus if we can compute the strain energy for a sample on whose boundary these displacements are imposed the effective area modulus is known. Similarly if we impose the displacements

$$\begin{aligned} u &= bx \\ v &= -by \end{aligned} \quad (A5)$$

the strain energy for a uniform material is

$$U = 2Gba \quad (A6)$$

and for a material with varying stiffness is

$$U = 2G^*ba \quad (A7)$$

Consider the material of Fig. 1. Taking advantage of its symmetries we need compute the strain energy only in the representative area ABCD, applying the boundary conditions of Equations A2 and A5 to calculate  $K^*$  and  $G^*$ , respectively. This was done using 312 triangular elements with the MS/NASTRAN finite element program. (See Fig. 6a.) For the material described in Fig. 2 there is no symmetry with respect to a horizontal line. Therefore we used a strip of width one-half a triangle base in the analysis (between lines AB and CD in Fig. 2). The boundary conditions were applied to a strip of five half-equilateral-triangle pairs (see Fig. 6b). Energy was recorded separately for each pair. In no instance did the energy for the extreme upper or lower pair vary by more than 5% for the stiffness ratios calculated (400:1 being the extreme

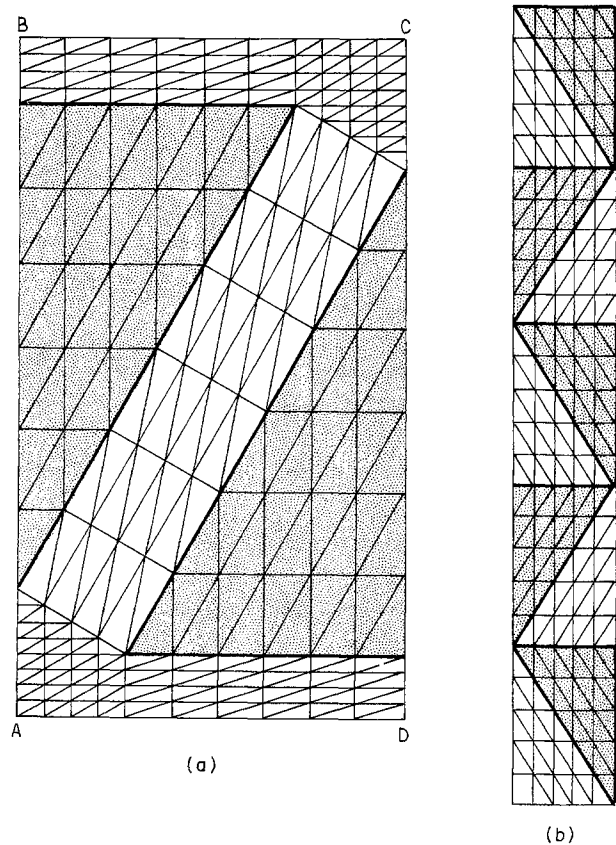


Figure 6 Grid for finite element analysis.

case). The energies calculated for the triangle pairs which bracketed the middle pair were almost indistinguishable from that of the latter. Therefore the energies of the middle pair of the five unit strip were used. Apparently the St Venant effect operates very quickly.

## References

1. H. L. COX, *Brit. J. Appl. Phys.* **3** (1952) 72.
2. P. LACACHEUX, *Papeterie* **75** (1953) 659.
3. O. J. KALLMES and G. A. BERNIER, in "The Formation and Structure of Paper", Transactions of the Symposium held at Oxford, Sept. 1961, edited by F. Bolam (Technical Section of the British Paper and Board Maker's Association, London, 1962) pp. 369-388.
4. R. W. PERKINS, Jr., Proceedings of 50th Anniversary Conference of the Institute of Paper Chemistry, Appleton, Wisconsin, 1980, pp. 89-111.
5. D. H. PAGE and R. S. SETH, *Tappi* **63** (1980) 113.
6. K. SCHULGASSER and D. H. PAGE, *Comp. Sci. Technol.* **32** (1988) 279.
7. H. CORTE, in "Handbook of Paper Science, Vol 2: The Structure and Physical Properties of Paper", edited by H. E. Rance, (Elsevier, Amsterdam, 1982) p.175.
8. H. CORTE, *Das Papier* **24** (1970) 261.
9. R. M. CHRISTENSEN, "Mechanics of Composite Materials", (Wiley, New York, 1979) p. 106 ff.
10. M. J. BERAN, "Statistical Continuum Theories", (Interscience, London, 1968) p. 222 ff.
11. Z. HASHIN, *J. Mech. Phys. Solids* **13** (1965) 119.
12. N. R. SILNUTZER, PhD Dissertation, University of Pennsylvania, Philadelphia, (1972) p. 128.
13. G. W. MILTON, "Modelling the Properties of Composites by Laminates", in "Homogenization and Effective Moduli of Materials and Media", edited by J. L. Erikson, D. Kinderletter, R. Kohn and J.-L. Lion, (Springer, Berlin, 1986) pp. 150-174.
14. K. SCHULGASSER, *Fibre Sci. Technol.* **19** (1983) 297.
15. O. KALLMES and H. CORTE, *Tappi* **43** (1960) 737.
16. B. RADVAN, C. DODSON and C. G. SKOLD, Transactions of the Symposium held at Cambridge, September

1965, edited by F. Bolam (Technical Section of the British Paper and Board Makers' Association, London, 1966) pp. 189-214.

17. B. D. JORDAN and N. G. NGUYEN, *Paperi ja Puu* **68** (1986) 476.
18. B. D. JORDAN, private communication.
19. H. CORTE and C. T. J. DODSON, *Das Papier*, **23** (1969) 381.

20. D. H. PAGE and R. S. SETH, *Tappi* **63** (1980) 108.

21. A. M. SCALLAN and J. BORCH, *Tappi* **55** (1972) 583.

*Received 9 February  
and accepted 24 August 1989*